

REPORT DOCUMENTATION PAGE

Form Approved
OMB No. 074-0188

Public reporting burden for this collection of information is estimated to average 1 hour per response, including the time for reviewing instructions, searching existing data sources, gathering and maintaining the data needed, and completing and reviewing this collection of information. Send comments regarding this burden estimate or any other aspect of this collection of information, including suggestions for reducing this burden to Washington Headquarters Services, Directorate for Information Operations and Reports, 1215 Jefferson Davis Highway, Suite 1204, Arlington, VA 22202-4302, and to the Office of Management and Budget, Paperwork Reduction Project (0704-0188), Washington, DC 20503

1. AGENCY USE ONLY (Leave blank)		2. REPORT DATE Jan. 1- Mar. 31, 1995	3. REPORT TYPE AND DATES COVERED Quarterly report, Jan. 1- Mar, 31, 1995	
4. TITLE AND SUBTITLE Kinetics of Supercritical Water Oxidation			5. FUNDING NUMBERS N/A	
6. AUTHOR(S) Steven F. Rice				
7. PERFORMING ORGANIZATION NAME(S) AND ADDRESS(ES) Sandia National Laboratories Combustion Research Facility MIT Princeton University			8. PERFORMING ORGANIZATION REPORT NUMBER Case 8610.000	
9. SPONSORING / MONITORING AGENCY NAME(S) AND ADDRESS(ES) SERDP 901 North Stuart St. Suite 303 Arlington, VA 22203			10. SPONSORING / MONITORING AGENCY REPORT NUMBER N/A	
11. SUPPLEMENTARY NOTES Prepared by Sandia National Laboratories, Combustion Research Facility, Case 8610.000. This work was supported in part by the US Army Armament Research Development and Engineering Center (ARDEC). The United States Government has a royalty-free license throughout the world in all copyrightable material contained herein. All other rights are reserved by the copyright owner.				
12a. DISTRIBUTION / AVAILABILITY STATEMENT Approved for public release: distribution is unlimited			12b. DISTRIBUTION CODE A	
13. ABSTRACT (Maximum 200 Words) This project consists of experiments and theoretical modeling designed to improve our understanding of the detailed chemical kinetics of supercritical water oxidation (SCWO) processes. The objective of the three year project is to develop working models that accurately predict the oxidation rates and mechanisms for a variety of key organic species over the range of temperatures and pressures important for industrial applications. Our examination of reaction kinetics in supercritical water undertakes <i>in situ</i> measurements of reactants, intermediates, and products using optical spectroscopic techniques, primarily Raman spectroscopy. Our focus is to measure the primary oxidation steps that occur in the oxidation of methanol, phenol, methylene chloride, and some simple organic compounds containing nitro groups with a special emphasis on identifying reaction steps that involve hydroxyl radical and hydrogen peroxide.				
14. SUBJECT TERMS supercritical water oxidation (SCWO), optical spectroscopic techniques, Raman spectroscopy, SERDP			15. NUMBER OF PAGES 20	
			16. PRICE CODE N/A	
17. SECURITY CLASSIFICATION OF REPORT unclass	18. SECURITY CLASSIFICATION OF THIS PAGE unclass	19. SECURITY CLASSIFICATION OF ABSTRACT unclass	20. LIMITATION OF ABSTRACT UL	

NSN 7540-01-280-5500

Standard Form 298 (Rev. 2-89)
Prescribed by ANSI Std. Z39-18
298-102

Kinetics of Supercritical Water Oxidation

SERDP Compliance Technical Thrust Area

Quarterly Report

Sandia National Laboratories
Combustion Research Facility
Case 8610.000



Principal Investigator: Steven F. Rice, SNL

Project Associates, SNL: Richard R. Steeper, Thomas B. Hunter,
Russell G. Hanush, Jason D. Aiken, Åsa Karlegård

Research Contractors: Jefferson W. Tester, MIT
Kenneth Brezinsky, Princeton University

Project Manager: Donald R. Hardesty

Reporting Period: January 1 -March 31, 1995

19980806 142

Project description:

This project consists of experiments and theoretical modeling designed to improve our understanding of the detailed chemical kinetics of supercritical water oxidation (SCWO) processes. The objective of the three year project is to develop working models that accurately predict the oxidation rates and mechanisms for a variety of key organic species over the range of temperatures and pressures important for industrial applications. Our examination of reaction kinetics in supercritical water undertakes *in situ* measurements of reactants, intermediates, and products using optical spectroscopic techniques, primarily Raman spectroscopy. Our focus is to measure the primary oxidation steps that occur in the oxidation of methanol, phenol, methylene chloride, and some simple organic compounds containing nitro groups with a special emphasis on identifying reaction steps that involve hydroxyl radical and hydrogen peroxide.

The work conducted here continues the experimental approach from our previous SERDP-funded project by extending measurements on key oxidant species and expanding the variety of experimental methods, primarily optical in nature, that can be used to examine reactions at SCWO conditions. Direct support will be sent to the project collaborators at MIT and Princeton who will contribute to the model development for the halogenated systems and phenol. In general, these researchers will examine these processes using more conventional sample and quench

methods. These experiments all focus on determining the primary oxidation steps that involve the OH and HO₂ radicals, generating data which will be used to evaluate and refine SCWO reaction kinetic schemes. The primary technical difficulty in this stage of the project will be recasting the 1100 °C models for these simple molecules to 400-600 °C emphasizing the role of the HO₂ radical.

Executive Summary of Progress this Period

Programmatic

During this quarter, the FY95 SERDP execution plan was submitted to the SERDP office. Requests for quotes were issued in early February to MIT and Princeton University for their project assignments. These contracts will initiate the participation of these two institutions on the project. MIT responded in March we expect a start date of 5/1/95. Princeton's contract office has been slow in responding and we expect a start date of 6/1/95. We are optimistic that a 6/1 start date is possible.

Methane oxidation

Work this quarter was directed at methanol and isopropanol and as a result only a small amount of activity was focused on methane oxidation. During this quarter, analysis of the methane oxidation results focused on the unusual pressure dependence that was observed for methane oxidation in water and on developing an explanation based on the kinetic scheme that can, at least, qualitatively account for the observations.

Methanol oxidation

Because of the success of the elementary reaction step model for methanol, we have begun to analyze the mechanism in more detail to identify the relationship between key elementary steps and the overall oxidation process. The modeling predictions suggest that a large amount of hydrogen peroxide is generated during the oxidation of methanol and that it is this production of hydrogen peroxide and subsequent unimolecular decomposition of H₂O₂ that effectively controls the oxidation of methanol.

Isopropanol oxidation

A series of flow reactor (SCWOFR) and constant-volume reactor (SCWO-VCR) experiments were performed on isopropanol to provide critically needed results for the DOE EM-50 project at INEL and for ARDEC-sponsored projects¹ in Sandia's

¹ This program is sponsored by the U.S. Army Armament Research Development and Engineering Center (ARDEC) at Picatinny Arsenal. Foster Wheeler Development Corp. is the A&E sub-contractor. The project goal is to build and operate a production prototype SCWO reactor using a platelet transpiring wall concept. The reactor will be located at Pine Bluff Arsenal and will be used for processing a variety of organic dyes used by the military.

Engineering for Transportation and Environment Dept. with Foster Wheeler Development Corporation. These data show that isopropanol is much more reactive than methanol, but undergoes a mechanistic step similar to methanol's partial oxidation to formaldehyde. At temperatures below 450 °C, isopropanol will rapidly oxidize to acetone, but that oxidation process slows dramatically and acetone appears in the Raman spectrum and in effluent gas chromatograms as the primary organic product of partial oxidation.

Hydrogen peroxide thermal decomposition

This quarter we initiated a sensitivity analysis on the kinetics model for methanol oxidation. Initial results indicate the importance of hydrogen peroxide in the oxidation process in supercritical water. A mobile, small-scale, optically accessible reactor was designed and fabrication is nearly completed. Special ultra-high-purity windows have been procured and a novel pressure let-down technique was developed to afford controlled flow at the exceptionally low flow rates required for this experiment.

Phenol oxidation and pyrolysis

Preliminary experiments were conducted in SCWOFR flow reactor on the oxidation and pyrolysis of phenol. The emphasis for these tests was to identify the relevant temperature/time range for oxidation, establish detection levels of phenol, and quantify the temperature ranges that pyrolysis reactions during reactant preheat can affect the oxidation measurements.

SERDP-leveraged tasks for platelet reactor design

A series of tests was completed to generate critical design data on the oxidation of military spotting dyes for the ARDEC-sponsored program in Sandia. Our task was to establish that the oxidation rates of typical dyes would be sufficiently high at industrial feed concentrations to be permit adequate waste destruction at the intended reactor operating temperatures. We established that the effective reaction rate at 5 wt% (dye in water initial concentration) was in fact higher than 0.5 wt% (of dye in water) at comparable temperatures. This result alleviated concerns that earlier feasibility studies may have possibly overpredicted the industrial-scale destruction efficiency.

Future work

Primary goals for next quarter are to complete and submit manuscripts for publication on the methanol work, the initial work on isopropanol, and the characterization of our experimental methods. In addition, we intend to complete the experimental work on isopropanol kinetics and extend the experiments to n-propanol.

Detailed Summary of Technical Progress this Period

Methane oxidation

Currently, the elementary reaction step model that reproduces experimental methanol oxidation rates does not accurately reproduce the observations for methane, especially the unusual pressure dependence that has been observed (see previous quarterly report). The elementary model does indicate, however, that the role of hydrogen peroxide is critical in determining the overall oxidation rate for methane, methanol, and formaldehyde. In the model, the thermal decomposition of H_2O_2 is described in the "high pressure limit" such that the reaction is written as being effectively first order and that pressure-dependent collisional effects are suppressed. As a result, it is not surprising that the elementary model does not represent pressure effects well. The experiments described below, on the direct measurement of H_2O_2 decomposition, should provide valuable insight on this issue.

Methanol oxidation

The focus on the methanol work this quarter was on comparison of our experimental results with the results from several elementary reaction models. The models developed elsewhere, including two developed by Pitz at LLNL [1,2] over the past several years and one developed by Webley [3]. We have found that the original Pitz (PITZ1) [1] model, does good job representing the data. The second Pitz model was developed to compare with the results of Holgate et. al. [4] for hydrogen oxidation and still represent the methanol results of Webley [3]. Since there is quantitative disagreement between the experimental results reported in Ref. 3 and ours, it is perhaps not surprising that this mechanism fails to reproduce our methanol oxidation results.

Figure 1 shows the results of the PITZ1 calculation in comparison with our experimental results for the disappearance of methanol. Figure 2 compares the results for the formation and subsequent disappearance of formaldehyde for the same set of experiments. The model represents the rate of the reaction quite well; the model predicts the chemistry to be only slightly slower than the observed rate. The model slightly underpredicts the peak formaldehyde concentration at all temperatures and fails to represent the experimental trend of increasing peak concentration with increasing reaction temperature.

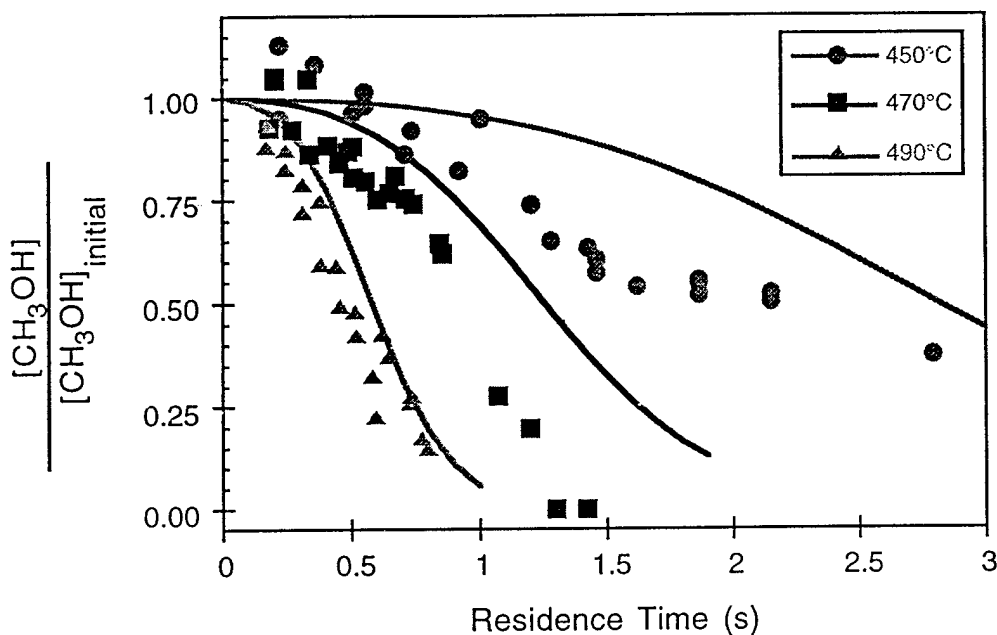


Figure 1. Comparison of the experimental results for oxidation of methanol at several temperatures under supercritical water conditions in Sandia's SCWOFR reactor with results based on the PITZ1 elementary reaction model.

The comparison suggests that agreement between the model and experiment would be improved if the effective rate for oxidation of methanol is increased, but the rate of oxidation of formaldehyde were left unchanged. This would serve to remove methanol from the system faster, producing better agreement with the experimental data. Simultaneously, a more rapid build up of formaldehyde would be predicted. It is not likely that changing any of the hydrogen/oxygen part of the mechanism would produce any effect. By modifying these reactions, transient populations of the key oxidizer radicals, OH and HO₂, would be changed, but these changes would affect the methanol and formaldehyde rates in a similar way. We suspect that the step $\text{CH}_3\text{OH} + \text{HO}_2 \Rightarrow \text{CH}_2\text{OH} + \text{H}_2\text{O}_2$, which is reported with large experimental error [2] is the reaction in the model needs to be corrected.

We are working closely with W.J. Pitz to resolve these issues. It is hoped that we can arrive at a model that can reproduce the H₂ measurements of Holgate, and also faithfully reproduce our new methanol results.

Isopropanol Oxidation

Two sets of experiments, designed to measure the rate of oxidation of isopropanol at temperatures ranging from 340 °C to 480 °C, were completed this quarter. These experiments were done to support Sandia's project to build a SCWO reactor for ARDEC at Pine Bluff Arsenal for destroying military dyes. The rate of isopropanol

oxidation at these temperatures is needed to properly design the reactant heat-up section of the production prototype reactor. This work was intended to generate rapidly much needed design data. Additional work on isopropanol and n-propanol will be done next quarter.

SC WO -CVR experiments

Our cell reactor is an optically accessible, constant volume, externally heated vessel (internal volume, 20 ml) designed to be used for measuring reaction rates that occur on the >20 s timescale. The experiments reported here covered the temperature range from 340 °C to 400 °C at a nominal pressure of 4000 psi. There was an approximately 300 - 800 psi pressure increase in the reactor due to the injection of the oxidizer depending on the initial starting pressure. The magnitude of this increase was difficult to predict *a priori* and, as a result, the seven experiments described here varied in final pressure from 3500 psi to 4200 psi.

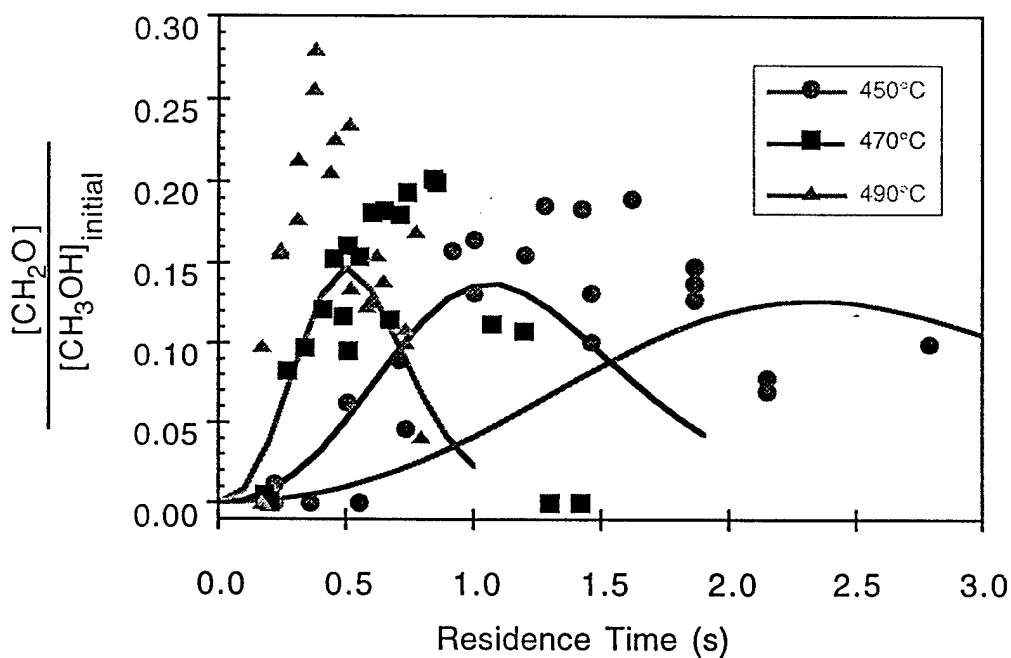


Figure 2. Comparison of the experimental results of the production and subsequent loss of formaldehyde during the oxidation of methanol at several temperatures under supercritical water conditions in Sandia's SCWOFR reactor and the results from the PITZ1 elementary reaction model.

We used Raman spectroscopy to monitor directly the concentration of isopropanol as a function of time. The Raman signal (which is proportional to isopropanol concentration), temperature, and pressure were continuously monitored. These individual Raman spectra were then analyzed to produce a measurement of remaining isopropanol vs. time.

A typical experiment followed these procedural steps: 1) a solution of 2 wt% isopropanol was injected into the preheated reactor and allowed to equilibrate at the preset reaction temperature, while the Raman signal was monitored to ensure that no pyrolysis occurred; 2) an 11 wt% H₂O₂ solution at ambient temperature was injected into the reactor over a period of approximately 15 seconds 3) Raman spectra of isopropanol were recorded every 10 seconds.

Table 1 presents the measured effective time constants of the reaction with temperature, where we define the effective time constant τ_{eff} as the time at which the concentration of isopropanol has decreased to 1/e of its original concentration. Note that the τ_{eff} for the higher temperature points are on the order of the oxidizer addition rate, and may represent a convolution of the reaction rate and the addition rate.

The temperature increase in the fluid detected for each run over a period of approximately t_{eff} is listed below. We note that this reactor is not an adiabatic system and these temperature increases are listed only for illustrative purposes to indicate that the rate of energy release is slow relative to heat transfer to the vessel walls.

Table 1. Results from Cell Reactor

Run #	T Initial (°C)	T Rise (°C)	τ_{eff} (s)
1	346	5	140
2	343	7	134
3	372	12	100
4	370	12	110
5	395	4	25
6	392	10	15
7	402	12	10

SCWOFR experiments

A second set of experiments was conducted this quarter in our optically accessible flow reactor, SCWOFR. This reactor is designed to examine reaction rates in the range of 0.15 - 5 s. In this system, the two reactant delivery lines, one for fuel and one for oxidizer, are simultaneously preheated and are joined to mix the feeds at a single point. By varying the reactant flow rates, and monitoring the reacting fluid at

a fixed point downstream, the amount of isopropanol remaining in solution can be monitored as a function of residence time in the reactor. In addition, we have the ability to monitor the presence of reaction intermediates. In this case we used a 2 wt% isopropanol solution and a 6 wt% solution of oxygen created from a heated H_2O_2 solution that is thermally decomposed into O_2 . The pressure for these experiments was 3550 psi.

Results from these experiments are presented in Figures 3 and 4. Note that the τ_{eff} at 402 °C from the cell reactor is in excellent agreement with the 400 °C results from the flow reactor. The results in Figure 3, produce a value of $\tau_{\text{eff}} = 10.3$ s based on a Fraction Remaining Fuel of $C/C_0 = 0.8$ at a reaction time of 2.3 s (where C is the concentration measured and C_0 is the initial feed concentration). The agreement here illustrates that the reaction in the cell from direct hydrogen peroxide feed may not be much faster than with oxygen. This is because the thermal decomposition of hydrogen peroxide proceeds much faster than the oxidation does and consequently H_2O_2 simply converts to O_2 on a much faster timescale than it reacts with the feed. We reiterate, however, that the H_2O_2 addition rate in the 402 °C experiment is comparable to the oxidation rate, such that the τ_{eff} of 10 s is only a very rough estimate. The values at 395 °C are more reliable.

Figure 4 shows the concentration of acetone as a function of residence time in the reactor. The value plotted, $C_{\text{ace}}/C_{0(\text{ipa})}$ is the ratio of the observed acetone concentration to the initial isopropanol feed concentration. These data illustrate the point that even when a significant amount of the isopropanol is removed, much of it has been converted only to acetone. Note that at the higher temperatures, as the acetone is beginning to oxidize as well, its concentration has gone through a maximum.

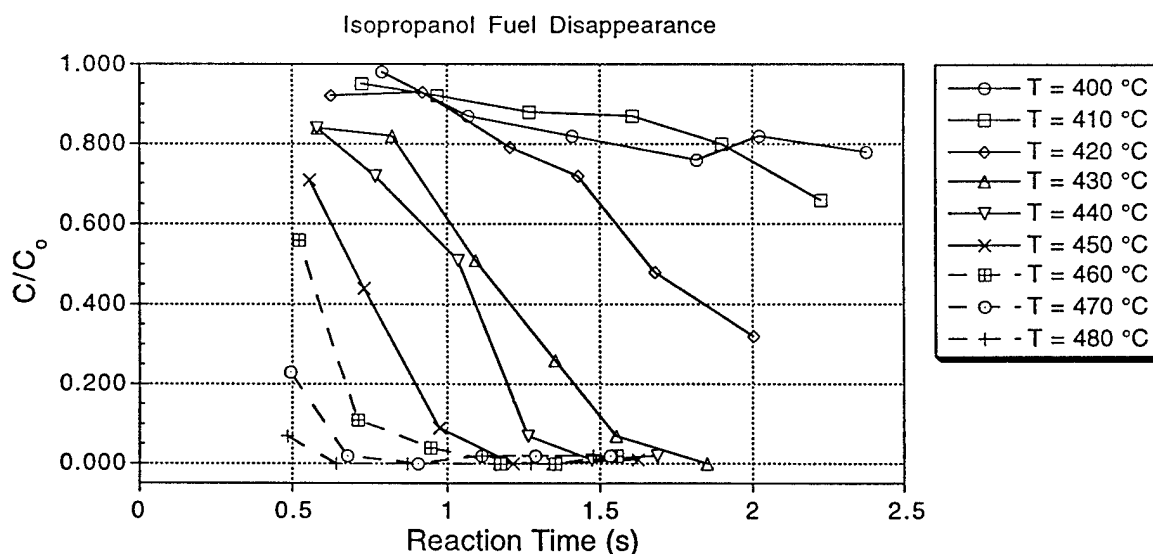


Figure 3. Measured isopropanol fraction remaining as a function of residence time.

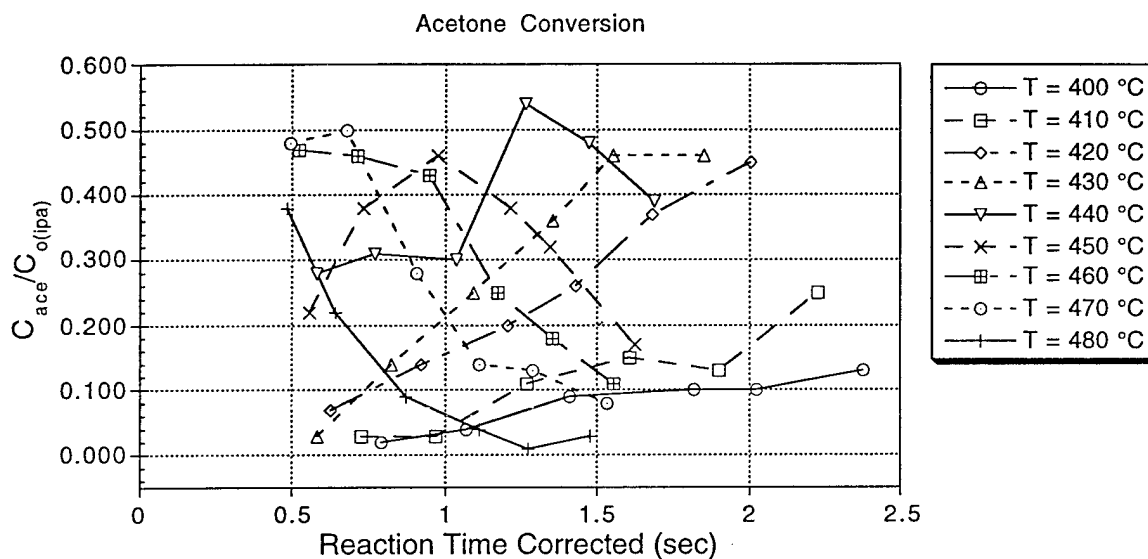


Figure 4. Measured fraction of isopropanol converted to acetone as a function of time.

Conclusions:

The results for the oxidation of isopropanol show that although it reacts rapidly relative to many organic species it will not serve as a rapid source of heat in a waste preheat system until the feed is already well above the critical temperature. It cannot react sufficiently rapidly to take a subcritical feed near 350 °C to well above the critical temperature in several seconds.

SERDP-leveraged tasks for platelet reactor

Sandia is presently involved in a project with the U.S. Army Armament Research Engineering and Development Center (ARDEC) at Picatinny Arsenal to fabricate and operate a supercritical water oxidation reactor at Pine Bluff Arsenal to destroy a variety of obsolete military smoke and dye compositions. The availability of the SCWOFR for the measurement of critical engineering design data has been important for the progress of this DoD project. We conducted three experiments to evaluate the destruction efficiency of acid orange dye at concentrations near those anticipated to be used for actual waste processing. The samples obtained from these tests were analyzed by total organic carbon (TOC) analysis. The samples have been retained and are available for additional analysis, if necessary.

Procedure

The SCWOFR flow reactor was configured identically to the configuration used for the ARDEC feasibility study. This is described in detail in "Supercritical Water Oxidation of Colored Smoke, Dye, and Pyrotechnic Compositions." SAND 94-8209 [5]. The general experimental procedure is described below.

A sample of acid orange dye was prepared at 9.38 wt% in water. The original goal was to prepare a sample at 10.0 wt%, but we found that the orange dye was not entirely dissolved at this loading at 23 °C. The oxidizer was 30 wt% H₂O₂ in water. Both the oxidizer and feed were pressurized and pumped at an ambient volumetric flow rate of 0.44 ml/s to produce a total flow rate of 0.88 ml/s of dye and oxidizer, and an approximate mass flow rate of 0.93 g/s. The temperature profiles of the reactor for the three runs are shown in Figure 5. When combined with the mass flow rate, density as a function of temperature, and the reactor cross section, the velocity can be calculated and then integrated to produce a time-temperature profile for each experiment. These are shown in Figure 6.

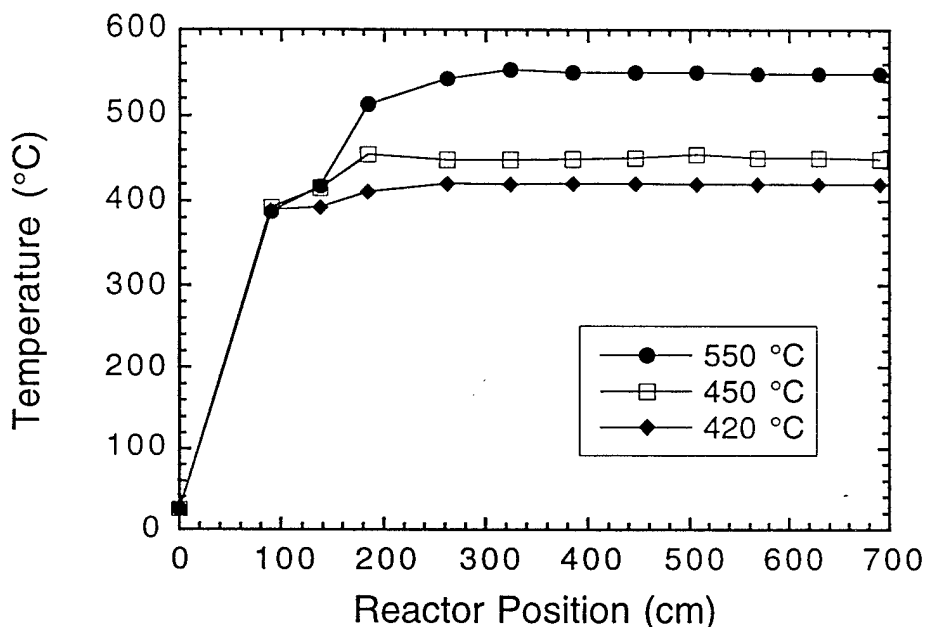


Figure 5. Temperature profile in the SCWOFR reactor for the acid orange dye experiments.

Each experiment was initiated by preheating the reactor to the desired initial temperature with only water flowing in the system. The oxidizer line was then switched to hydrogen peroxide and the system was allowed to equilibrate again. The feed line was then switched to dye and samples were taken at one minute intervals. There is a significant time delay in the feed line before the dye reaches the reactor. Consequently, the first few samples represent a "baseline" of only oxidizer. On the 550 °C run, the samples were collected until $t = 20$ minutes, when the first indications occurred of a pressure drop in the system due to accumulation of sodium sulfate deposits. The dye feed was immediately terminated. Samples were collected for another 5 minutes. For the 450 °C experiment, samples were collected

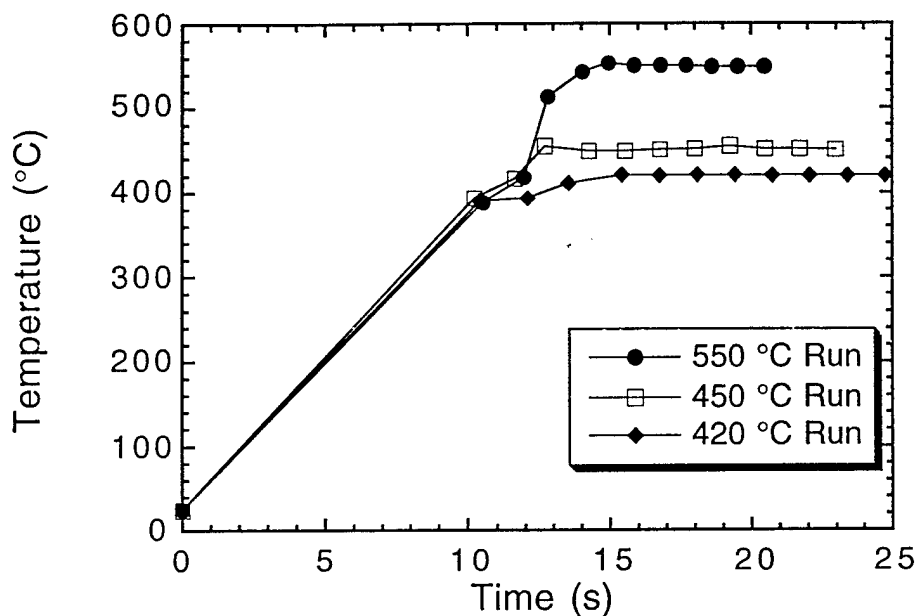


Figure 6. Time - temperature profile of the fluid in the SCWOFR reactor for the acid orange dye experiments.

in the same manner for 14 minutes with the dye on and a subsequent 6 minutes with the dye off. At 420 °C, the dye was on for 15 minutes followed by 10 minutes of rinsing. The results from the experiment are listed in Table 2.

The measured input Total Organic Carbon (TOC) was 27,000 ppm in the feed tank. This produces a TOC value for unreacted material to be 13,500 ppm, when diluted by the oxidizer. The calculated TOC for the feed tank based on 9.3 wt% should have been 39,500, not 27,000. A calibration sample of 0.1022 g dye in 100 ml was prepared and it registered 280 ppm (not 430 ppm as it should have based on the molecular formula). We believe that there is a considerable amount of water of hydration in the dye such that the correct formula for the dye is $C_{16}H_{10}N_2Na_2O_7S_2 \cdot n H_2O$, where $n = 12-14$. It is not unusual for salts of organic acids to include large amounts of water in the crystal lattice.

The table shows that the effluent began to show the presence of the dye at about five minutes and reached a steady state at about eight minutes. At 550 °C and 420 °C, samples were collected for sufficient time to allow the system to return nearly to pure organic - free effluent. The collection for the 450 °C run was terminated before the effluent completely returned to normal.

By averaging the "steady state" output at the three temperatures, and dividing by the input TOC (13,500), we can calculate a Destruction Removal Efficiency (DRE) for the three temperatures. Using 4.55 ppm, 631 ppm, and 816 ppm for 550 °C, 450°C, and 420 °C respectively, we calculate DREs of 94%, 95%, 99.96%. The effective residence times are determined from Figure 2 to be approximately 6.4, 8.7 and 9.3 seconds for 550 °C, 450 °C and 420 °C respectively.

We can compare these results to results reported earlier [5]. In Ref. 5, the orange dye is processed at various temperatures using oxygen as the oxidizer. By reducing the results to an effective first order rate constant, k_{eff} , the oxidation reaction rate is expressed as

$$d(\text{TOC})/dt = -k_{eff}(\text{TOC}).$$

Table 2. Total Organic Carbon in Effluent

Time (min)	TOC _{out} (ppm) 550 °C	TOC _{out} (ppm) 450 °C	TOC _{out} (ppm) 420 °C
1	2.3	1.5	5.6
2	2.1	1.8	3.9
3	2.2	0.78	4.2
4	1.9	2.9	3.4
5	4.1	50.4	62.6
6	5.4	308	496
7	2.9	312	741
8	5.9	335	834
9	4.7	531	814
10	4.5	559	830
11	4.0	659	802
12	4.5	611	819
13	4.7	586	853
14	4.7	622	822
15	4.4	653	802
16	5.2	748	797
17	5.4	718	789
18	9.9	517	722
19	5.3	99.3	656
20	6.7	15.3	144
21	6.0	-	31
22	5.5	-	12.1
23	9.8	-	5.9
24	2.2	-	4.8
25	2.0	-	4.3

Integrating this yields,

$$\ln(\text{TOC}_{\text{out}}/\text{TOC}_{\text{in}})/\tau = -k_{\text{eff}}$$

where (TOC) is the concentration of TOC in the system, and τ is the effective residence time. The results from Ref. 5 and our new experiments are consolidated in Figure 7.

The results shown in Figure 7 reveal that the effective reaction rate is faster in the new experiments where the dye feed was an order of magnitude higher and the oxidizer was hydrogen peroxide. This enhancement of reaction rate was more significant at low conversion than at high conversion. At this stage, we cannot conclusively determine whether this enhancement is due to the presence of hydrogen peroxide as the initial oxidizer, or if this is an effect due to increased fuel concentration. We suspect it is the latter, since in this configuration all of the H_2O_2 is converted to O_2 before the reactor temperature increases above about $300\text{ }^\circ\text{C}$ which is well below any temperature at which significant oxidation would occur. We should point out that we observe this effect of enhanced rate at high fuel loading for both methanol and methane oxidation.

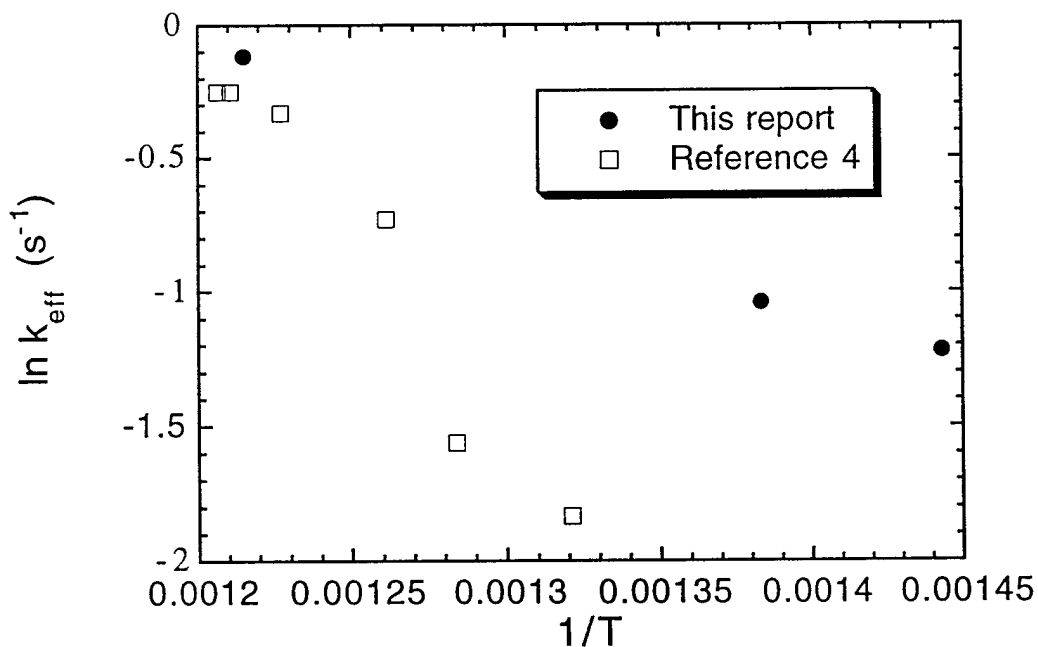


Figure 7. Arrhenius plot of the result for the oxidation of acid orange dye

Conclusions

These results show that waste mixtures as high as 5 wt% dye can be processed by SCWO with high destruction efficiencies and short residence times. The results also show that the effect of high concentrations of fuel and/or the addition of hydrogen peroxide increases the oxidation rate at low conversion, but has a lesser effect at high conversion. We believe, with some reservation, that it is the increased waste feed loading that produces the higher rates. We are certain that an increased fuel loading will not lead to a decrease in conversion efficiency. However, in order to take full advantage of these results, and to more fully understand these fuel loading effects, more investigation may be required.

Hydrogen peroxide thermal decomposition

This quarter we have established computationally that our proposed experimental method using pulsed-u.v.-laser photolysis of a solution of N₂O in supercritical water combined with transient absorption detection of reaction products should provide accurate chemical kinetic data on the thermal decomposition of hydrogen peroxide at high temperature and high density. These experiments will be conducted with P. Paul of Sandia's Diagnostic and Reacting Flow Department.

The proposed experimental procedure is to preheat and pressurize a solution of N₂O in water to the experimental conditions of 250 bar and 450 °C in a flow system equipped with an optical cell. This solution should be stable for many minutes providing ample time to reach steady P-T conditions. An Ar-F excimer laser operating at 193 nm will be used to photolyze the N₂O producing O ¹D atoms which will react with water (and recombine) to produce a solution of H₂O₂, O₂, and N₂ in supercritical water in about 10 μs. The H₂O₂ is unstable and will continue to decompose to water and molecular oxygen on a 10⁻³ - 10⁰ s timescale. This decomposition can be monitored by u.v. transient absorption spectroscopy at 240-200 nm. We expect to be able to produce 3x10⁻⁵ moles/liter H₂O₂, which will produce a steady state concentration of OH of 5x10⁻⁶ moles/liter (estimated). The goal of this experiment is to determine this value accurately.

Table 3: Key reactions in N₂O U.V. Photolysis in Supercritical Water

Photolysis Reactions:	Timescale
N ₂ O => N ₂ + O(¹ D)	10 ⁻⁸ s
O(¹ D) + H ₂ O => 2 OH	10 ⁻⁶ s
O + O + M => O ₂ + M	10 ⁻⁶ s (side reaction)
OH + OH + M => H ₂ O ₂ + M	approx. 5 x 10 ⁻⁶ s
Thermal decomposition route:	
H ₂ O ₂ => OH + OH	10 ⁻³ - 10 ⁰ s
OH + H ₂ O ₂ => H ₂ O + HO ₂	<10 ⁻³ s
HO ₂ + HO ₂ => H ₂ O ₂ + O ₂	<10 ⁻³ s

This method will provide for the production of H_2O_2 at temperature and pressures of interest in 10^{-6} seconds. Subsequent monitoring of the H_2O_2 concentration at 220 nm by transient absorption occurs on a much longer times scale. We have determined that absorption from the photolysis side products, O_2 , N_2 , HO_2 , OH , and of course H_2O , will not interfere with the experiment.

The flow reactor has been constructed and ultra pure sapphire windows have been procured. We anticipate beginning the experiment during the last quarter of FY95.

Phenol oxidation

Finally, this quarter, preliminary experiments were initiated to explore the applicability of the Raman spectroscopic method to the oxidation of phenol. The goals of this experiments were to: 1) determine the appropriate temperature/time range for the experiments; 2) ensure that phenol pyrolysis/hydrolysis reactions are sufficiently slow at these conditions to allow for the operation of the flow reactor in its standard configuration; and 3) establish phenol detectability levels using the Raman spectroscopic method.

A typical spectrum of the 1010 cm^{-1} band (the aromatic ring breathing mode) of phenol is presented in Figure 8. The feature is fairly strong and sharp, providing for excellent molecular detection specificity - because of the narrow linewidth, it will be relatively easy to distinguish phenol from other aromatics that may be produce in the reactor.

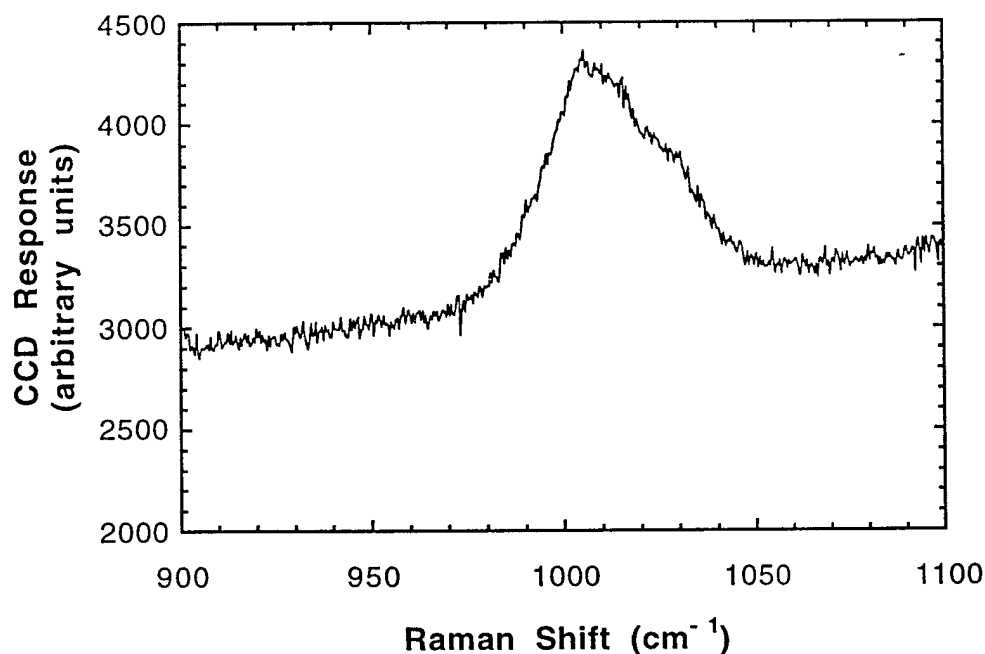


Figure 8. Typical Raman signal obtained from 1 wt% phenol in supercritical water.

The results from these preliminary experiments are presented in Table 4. The first four rows show the results from several pyrolysis experiments over the temperature range from 400 - 500 °C. The results show that the phenol is not pyrolyzing in the preheater. The last three rows show the results from several experiments conducted at different flow rates at 470 °C in the presence of oxygen. Because the residence time varies by a factor of three, if any oxidation were occurring at 470 °C, a distinct trend would be observed showing significantly less phenol present at the 1.44 s residence time point. Although there is considerable scatter in the data due to short scan times, at these short residence times, no detectable disappearance of phenol is observed. This observation is consistent with earlier measurements on phenol and indicates that much of the phenol oxidation experiments will need to be done at temperatures in excess of 500 °C.

Table 4. Phenol Oxidation and pyrolysis

T (°C)	Residence Time (s)	Fraction phenol remaining	Reaction
400	9.1	1.00	pyrolysis
450	6.9	1.02	pyrolysis
470	6.3	1.01	pyrolysis
495	4.4	1.02	pyrolysis
471	1.44	1.03	oxidation
473	0.86	1.05	oxidation
473	0.47	1.00	oxidation

Plans for next quarter

During the next quarter, we will complete the data analysis and submit manuscripts for publication on the methanol work, the initial work on isopropanol, and the characterization of our experimental methods. We will also complete the experimental work on isopropanol and extend the experiments to n-propanol and initiate the hydrogen peroxide experiments. We intend to implement key improvements to the flow reactor and its optical system, including: 1) upgrade the laser used for Raman spectroscopy, and 2) provide for the capability to deliver gaseous reactants to the flow reactor by adding a compressor for the feed line.

References

1. Schmitt, R. G.; Butler, P. B.; Bergan, N. E.; Pitz, W. J.; Westbrook, C. K. Destruction of Hazardous Waste in Supercritical Water. Part II: A Study of High-Pressure Methanol Oxidation Kinetics. 1991 Fall Meeting of the Western States Section/The Combustion Institute, University of California at Los Angeles, CA, 1991, 19.

2. M.K. Alkan, V.M. Pai, P.B. Butler, and W.J. Pitz, "Methanol and Hydrogen Oxidation Kinetics in Water at Supercritical States", submitted to *Combustion and Flame* (1995).
3. a) P.A. Webley, "Fundamental Oxidation Kinetics of Simple Compounds in Supercritical Water", Doctoral Thesis, Massachusetts Institute of Technology, Cambridge, MA (1989). b) J.W. Tester, P.A. Webley, and H.R. Holgate, "Revised Global Kinetic Measurements of Methanol Oxidation in Supercritical Water", *Ind. Eng. Chem. Res.*, **32**, 236 (1993).
4. a) H.R. Holgate and J.W. Tester, "Fundamental Kinetics and Mechanisms of Hydrogen Oxidation in Supercritical Water" *Combustion Science and Technology*, **88**, 369 (1993). b) H. R. Holgate and J. W. Tester, "Oxidation of Hydrogen and Carbon Monoxide in Sub- and Supercritical Water: Reaction Kinetics, Pathways, and Water Density Effects. 2. Elementary Reaction Modeling", *J. Phys. Chem.*, **98**, 810 (1994).
5. S.F. Rice, C.A. LaJeunesse, R.G. Hanush, J.D. Aiken, and S.C. Johnston, "Supercritical Water Oxidation of Colored Smoke, Dye, and Pyrotechnic Compositions", Sandia Report SAND94-8209 (1994).

Dr. E. Fenton Carey, Jr.
U.S. Department of Energy (ST-60)
1000 Independence Avenue, S.W.
Room GA 155
Washington, DC 20585

Dr. Robert Marianelli
U.S. Dept. Of Energy
19901 Germantown Rd.
Germantown, MD 20874

Jim Hurley
US AF AL/EQS
139 Barnes Drive, Suite 2
Tyndall Air Force Base, FL 32403

Dr. Peter Schmidt
Office of Naval Research
Chemistry Division
800 North Quincy Street
Arlington, VA 22217-5660

Dr. Robert Shaw
Chemical & Biological Sciences Div.
U.S. Army Research Office
Research Triangle Park, NC 27709-2211

Prof. Martin A. Abraham
The University of Tulsa
Department of Chemical Engineering
600 South College Avenue
Tulsa, OK 74104-3189

Prof. Joan F. Brennecke
University of Notre Dame
Department of Chemical Engineering
Notre Dame, IN 46556

Dr. Kenneth Brezinsky
Dept. of Mechanical and Aerospace
Engineering
Princeton University
PO Box CN5263
Princeton, NJ 08544-5263

Prof. Klaus Ebert
Kernforschungszentrum Karlsruhe
Institut für Heiße Chemie
Postfach 3640
D-76021 Karlsruhe
Germany

Prof. Earnest F. Gloyna
University of Texas at Austin
Environmental and Health
Engineering
Austin, TX 78712

Prof. Phillip E. Savage
University of Michigan
Chemical Engineering Department
Herbert H. Dow Building
Ann Arbor, MI 48109-2136

Carl Adema
SERDP Program Office
Program Manager for Compliance and
Global Environmental Change
901 North Stuart Street, Suite 303
Arlington, VA 22203

Trienel Ahearn
Labat-Anderson Incorporated
8000 Westpark Dr.
Suite 400
McLean, VA 22102

K.S. Ahluwalia
Foster Wheeler Development
Corporation
Engineering Science & Technology
12 Peach Tree Hill Road
Livingston, NJ 07039

Dr. Steven J. Buelow
CST-6
Los Alamos National Lab.
Los Alamos, NM 87545

Ernest L. Daman
Foster Wheeler Development
Corporation
12 Peach Tree Hill Road
Livingston, NJ 07039

Philip C. Dell'Orco
Los Alamos National Laboratory
Explosives Technology & Safety C920
Los Alamos, NM 87545

John Harrison
SERDP Program Office
901 North Stuart Street, Suite 303
Arlington, VA 22203

Dr. David A. Hazelbeck
General Atomics
M/S 15-100D
3550 General Atomics Court
San Diego, CA 92121-1194

Dr. Glenn T. Hong
MODAR, Inc.
14 Tech Circle
Natick, MA 01760

W. Killilea
MODAR, Inc.
14 Tech Circle
Natick, MA 01760

Richard Kirts
Naval Civil Engineering Laboratory
560 Laboratory Dr.
Port Hueneme, CA 93043-4328

Richard C. Lyon
Eco Waste Technologies
2305 Donley Drive
Suite 108
Austin, TX 78758-4535

Dr. Michael Modell
Modell Environmental Corporation
300 5th Avenue, 4th Floor
Waltham, MA 02154

Prof. Jean Robert Richard
CNRS
Combustion Laboratory
1C Avenue de la Recherche Scient.
Orleans 45071
France

Crane Robinson
Arament Research
Development & Engineering Center
(ARDEC)
SMCAR-AES-P
Building 321
Picatinny Arsenal, NJ 07806-5000

Dr. Gregory J. Rosasco
Nat'l Institute of Standards and
Technology
Division 836, Bldg. 221, Rm B-312
Gaithersburgh, MD 20899

Prof. Jefferson W. Tester
Massachusetts Institute of Technology
Energy Laboratory
Room E40-455
77 Massachusetts Avenue
Cambridge, MA 02139

Phil Whiting
Abitibi-Price Inc.
2240 Speakman Drive
Mississauga, Ontario L5K 1A9
Canada

Marvin F. Young
Aerojet
PO Box 13222
Sacramento, CA 95813-6000

MS0756 G.C Allen, 6607

MS9404 B. Mills, 8713

MS9001 T.O. Hunter, 8000
Attn: D.L. Crawford, 1900
E.E. Ives, 5200
M.E. John, 8100
L.A. West, 8600
R.C. Wayne, 8700

MS9054 W.J. McLean, 8300

MS9051 L. Rahn, 8351

MS9055 F. Tully, 8353

MS9056 G. Fisk, 8355

MS9052 D.R. Hardesty, 8361
Attn: Allendorf, S
Allendorf, M
Baxter, L

MS9052 J. Aiken, 8361

MS9052 R. Hanush, 8361

MS9052 T. Hunter, 8361

MS9052 S. Rice, 8361

MS9053 R. Steeper, 8362

MS9053 R. Carling, 8362

MS9053 C. Hartwig, 8366

MS9105 L.A. Hiles, 8400

MS9406 B. Haroldsen, 8412

MS9406 H. Hirano, 8412

MS9406 C. LaJeunesse, 8412

MS9406 M.C. Stoddard, 8412